Chemistry–A European Journal
Research Article
doi.org/10.1002/chem.202403239
Chemistry Europe
European Chemical Societies Publishing
www.chemeurj.org

Chirality at Metal in a Linear $[Ag(NHC)_2]^+$ Complex: Stereogenic C–Ag–C Axis, Atropisomerism and Role of π-π Interactions

Alvaro Polo,[a] Lara Gutiérrez Merino,[a] Ricardo Rodríguez,[a] and Pablo J. Sanz Miguel*[a]

Dedicated to Dr. Gabriele Trötscher-Kaus on the occasion of her retirement from TU Dortmund

Chirality at the metal center is a well-established concept, exemplified by numerous four- and six-coordinated complexes. Here, a pioneering example of linear chirality-at-metal is described: $[Ag(NHC)_2]^+$ (NHC = N-heterocyclic carbene). In solution, stabilizing π-π interactions preserve the chiral information of the solid state. Consequently, a novel class of atropisomers is identified, whose stereogenicity arises from hindered rotation around a C–Ag–C axis, instead of a typical C–C bond.

Introduction

Atropisomers are conformers that arise from restricted rotation around a single bond,[1] typically C–C, although an increasing number of molecules exhibiting C–N or N–N stereogenic axes have been reported.[2] First described a century ago,[3] the study of their properties has fascinated generations of scientists. Naturally occurring atropisomers are frequently exploited in medicinal chemistry.[4] In this regard, many efforts are being made also to design and improve atropisomeric drugs,[5] catalysts,[6] luminescence emitters,[7] or molecular machines,[8] to name a few.

Additionally, chiral-at-metal complexes, where the coordination of achiral ligands to metal centers determines the resulting chirality, are well established. Most examples involve octahedral coordination complexes, while tetrahedral and square-planar arrangements are less common.

In octahedral configurations, substantial contributions of Meggers,[9] and others[10] have expanded the conceptual horizons of metal-centered chirality applications. Regarding four-coordinated geometries, Zn and Ni complexes of Shionoya are noteworthy.[11] Other notable examples include tetrahedral chirality-at-silver in DNA metal-mediated base pairs[12] reported by Müller,[13] the square-planar chiral-at-Pt complexes exhibiting phosphorescence in solution and solid state described by Clever,[14] or the Umakoshi's photoluminescent chiral-at-cluster (Ag,Pt) systems.[15] To the best of our knowledge, chiral-at-metal complexes with a linear coordination geometry have not yet been reported.

Here, we present a pioneering linear chiral-at-metal complex, $[Ag(NHC)_2]^+$ (NHC = N-heterocyclic carbene), which encloses a silver ion and two symmetric NHC ligands, displays a stereogenic C–Ag–C axis, and exhibits a singular case of atropisomerism, even in solution state.

Results and Discussion

In the first step of ligand synthesis (Scheme 1), theophylline (HTheo) was converted to 7-(hydroxymethyl)theophylline and then to 7-(chloromethyl)theophylline (**1**). Further reaction of the latter with imidazole (HIm) leaded to Theo-CH_2-Im (**2**), variating a method by Hahn.[16] This was followed by the incorporation of a second nucleobase framework to the system. To that end, reaction of **2** with **1** was carried out in refluxing acetonitrile, yielding the corresponding imidazolium derivative [Theo-CH_2-Im-CH_2-Theo]Cl (**3**H[Cl]).

The NHC proligand (**3**H[Cl]) exhibited poor solubility in organic solvents, hindering the synthesis of the subsequent

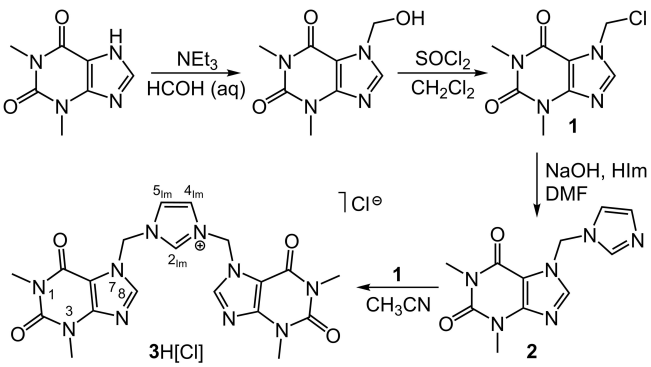

Scheme 1. Synthesis of **3**H[Cl], and ^{1}H NMR numbering schema.

[a] A. Polo, L. Gutiérrez Merino, R. Rodríguez, P. J. Sanz Miguel
Departamento de Química Inorgánica, Instituto de Síntesis Química y Catálisis Homogénea (ISQCH), Universidad de Zaragoza-CSIC, 50009 Zaragoza, Spain
E-mail: pablo.sanz@unizar.es

Supporting information for this article is available on the WWW under https://doi.org/10.1002/chem.202403239

Ag^+ complex. Consequently, an anion exchange reaction was performed, replacing the chloride anion with hexafluorophosphate in aqueous media by adding NH_4PF_6. As a result, **3**H[PF_6] was precipitated and isolated after several washings with methanol. Slow evaporation of the mother liquor yielded the adduct **3**H[PF_6]·CH_3OH, whose solid state structure was determined by X-ray crystallography. In solution, cation [Theo-CH_2-Im-CH_2-Theo]$^+$ (**3**H$^+$) can adopt different conformations, as rotation of both Theo fragments around the -CH_2- bridges is possible.

The ^{1}H NMR spectrum of **3**H[PF_6] in CD_3CN (*vide infra*) reveals a symmetric pattern on the NMR time scale. The signal at lowest field corresponds to $H2_{Im}$ of the imidazole ring (9.36 ppm), followed by H8 of theophylline (8.05 ppm). Both $H4_{Im}$ and $H5_{Im}$ protons exhibit an identical shift (7.66 ppm) owed to molecular symmetry. The proton signals assigned to -CH_2- bridges (6.50 ppm) and *N3*- and *N1*- methyl groups (3.44 ppm and 3.24 ppm, respectively) complete the spectrum.

The solid state structure of **3**H[PF_6]·CH_3OH[17] reveals a mutual *head*$_{(Theo)}$-*tail*$_{(Im)}$-*head*$_{(Theo)}$ (C8a/$C2_{Im}$/C8b)[18] aligning of the three imidazole rings (Figure 1). Bond lengths and angles are within the expected ranges. Interestingly, cation **3**H$^+$ is twisted in such a way that the PF_6^- anion remains wrapped in a host-guest fashion, with the resulting loss of (C_s) symmetry. Three *fac*-positioned F atoms of PF_6^- interact with the rings of the Theo fragments. Distances from F11 to the best pyrimidine planes are 2.918(1) Å (ring A) and 3.228(1) Å (ring B), while F12 and F13 point toward the imidazole rings A (2.998(1) Å) and B (2.982(1) Å), respectively. Thus, stabilization of the host-guest system occurs via multiple anion-π interactions, in combination with the expected Coulombic attraction. In view of the NMR spectra (see Supporting Information), configurations are not maintained in solution.

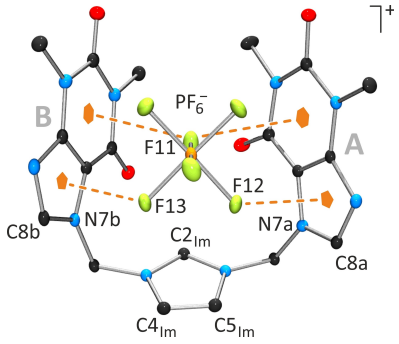

Figure 1. Host-guest interactions involving PF_6^- and cation **3**H$^+$ in the crystal packing of **3**H[PF_6]·CH_3OH.

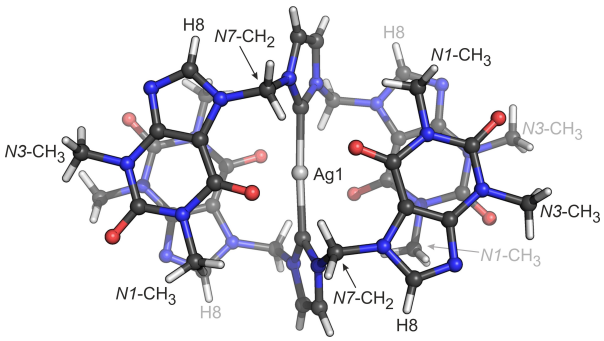

Figure 2. Front view of cation **4** (S_a enantiomer) in **4**[PF_6].

The title compound has been prepared by reacting a solution of **3**H[PF_6] in acetonitrile with Ag_2O under mild conditions.[19] Upon deprotonation of **3**H$^+$ (namely, **3**), and subsequent coordination of Ag^+, the NHC complex [Ag(**3**)$_2$][PF_6], hereinafter **4**[PF_6], was obtained.

X-ray crystallography revealed cation **4**[17] to be a linear complex in which both NHC (**3**) ligands are symmetry related (Figure 2). The C2–Ag1–C2′ angle is 176.98(14)°, whereas Ag1–C2 bond distances are 2.087(3) Å.[20] As expected, coordination of silver to both C2(NHC) atoms entails changes in the geometry of the ligands and their electron distribution.[21] In particular, the most remarkable alteration owed to the formal substitution of a Ag^+ ion for a proton is the decrease of the $N1_{Im}-C2_{Im}-N3_{Im}$ angle: from 107.82(11)° in **3**H[PF_6]·CH_3OH, to 103.4(2)° in **4**[PF_6]. Dihedral angles between imidazole and theophylline fragments of the same **3** ligand are 74.45(11)° and 77.87(11)°, whereas both symmetry related imidazole rings are tilted 48.32(10)°.

Regarding the spatial arrangement of ligands **3** in cation **4**, the following points are noteworthy: On one hand, the imidazole fragments in **4** are oriented *head*$_{(Theo)}$-*tail*$_{(Im)}$-*head*$_{(Theo)}$ (Figure 3), similar to the arrangement in cation **3**H$^+$. Conversely, while **3**H$^+$ exhibits a twisted U-conformation, both NHC ligands in **4** are arranged in a Z fashion (Figure 3). It should be noted that the highest symmetry of the Z-conformation for this ligand is C_2, and it exists as two enantiomers (R_a and S_a). Thus, the formation of cation **4** requires both **3** ligands to be homochiral and to adopt a Z geometry around the silver center (Figure 3).

Consequently, the spatial arrangement of both **3** NHC ligands in **4**[PF_6] defines its chirality. To distinguish between the two enantiomers of **4**, a similar approach to that used for BINAP

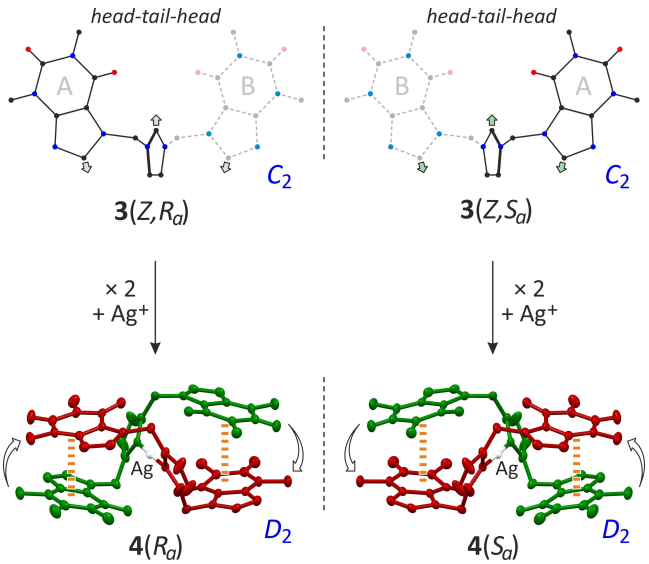

Figure 3. Conceptual depiction of the chiral organization of cation **4**. π-π interactions (3.6–3.9 Å) are highlighted in orange.

(2,2′-bisdiphenylphosphino-1,1′-binaphthyl) was employed for the stereogenic C2–Ag–C2′ axis. Both **4**(R_a) and **4**(S_a) enantiomers were identified in the crystal lattice (Figure 3). Chiral resolution through the formation of a diastereomeric mixture upon combination with a variety of chiral anions, such as camphor sulfonate, binaphthyl phosphate, and bis(binol) borate[17,22] was unsuccessful, meaning that **4**(R_a) and **4**(S_a) could not be isolated separately.

The Z arrangement of both homochiral NHC ligands in cation **4** is stabilized via twofold π-π interactions between nucleobases. Both A···A′ and B···B′ pyrimidine fragments are stacked in an antiparallel fashion. Another remarkable aspect is that O6a (0.245(3) Å) and O6b (0.134(3) Å) sites are situated out of their respective best nucleobase planes, moving away from the Ag^+ center, up to separations of 2.989(2) Å and 3.052(2) Å, respectively (Figure 4). Thus, both oxygen atoms remain outside the metal coordination sphere. Consequently, since no significant Ag···O interactions can be expected, the geometry of cation **4** is strictly linear. This observation can be explained by the strong σ-donating nature of the NHC ligands, which decreases the Lewis acidity of the silver ion and prevents additional interactions.[19a]

Since the solid state structure of **4**[PF_6] revealed stabilizing π-π stacking that keeps the ligands in close proximity, additional NMR experiments were performed in order to determine whether this atropisomeric arrangement is maintained in solution.

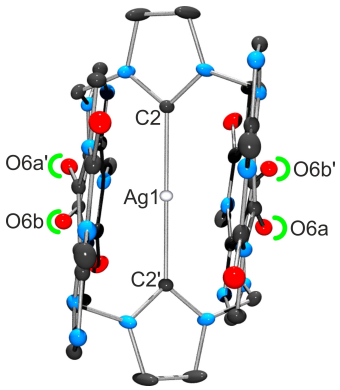

Figure 4. Side view of cation **4**.

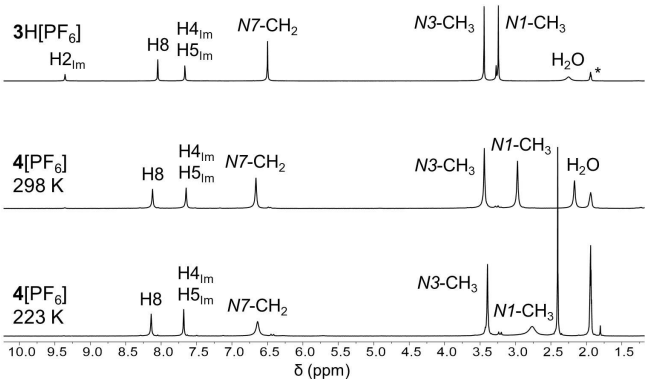

Figure 5. ^{1}H NMR spectra (CD_3CN) of **3**H[PF_6] (298 K) (top), **4**[PF_6] (298 K) (middle), and **4**[PF_6] (223 K) (bottom). Asterisk (*) denotes solvent residual peak.

Silver coordination to both **3** ligands in **4** was confirmed by NMR spectroscopy (Figure 5). In solution, cation **4** exhibits its highest symmetry (D_2) on the NMR time scale. At room temperature, the ^{1}H NMR spectrum of **4**[PF_6] shows a pattern similar to that of **3**H[PF_6], except for the disappearance of the $H2_{Im}$ signal. The signals attributed to the *N7*-CH_2 methylene bridges displayed downfield shifts ($\Delta\delta$ = 0.16 ppm), due to the closeness of the Ag^+ ion. Conversely, the *N1*-CH_3 proton signals are substantially upfield shifted ($\Delta\delta$ = 0.27 ppm), owed to the proximity of the aromatic ring current. Note that in **4**[PF_6], the X-ray crystallographic distance from C1a to the best imidazole plane is 3.605(4) Å.

At 223 K, the ^{1}H NMR spectrum (Figure 5) displays an additional upfield shift ($\Delta\delta$ = 0.48 ppm relative to **3**H[PF_6]) of the *N1*-CH_3 signal, consistent with an increased level of interaction between these methyl groups and the imidazole rings. In addition, clear broadening of the *N7*-CH_2 and the *N1*-CH_3 proton signals is observed, with the effect being more pronounced for the latter. In both cases, this effect is further attributed to the slowing down of intramolecular flapping and/or rotation, and therefore, *N7*-CH_2 protons become diastereotopic.

More importantly, NOESY experiments at 223 K (Supporting Information, Figure SI-31) are consistent with our interpretation of the ^{1}H NMR spectra and confirm the atropisomeric behavior of cation **4** in solution. The observed NOESY close correlations between *N1*(CH_3)-*N7*(CH_2), *N1*(CH_3)-H(4,5), *N1*(CH_3)-H8, *N7*(CH_2)-H(4,5), and *N7*(CH_2)-H8, are only consistent if both NHC ligands are arranged in a Z fashion and if π-π interactions are maintained in solution. Interconversion between enantiomers was not detected by NMR spectroscopy, though this does not preclude its occurrence on a small scale.

Conclusions

In summary, we synthesized a symmetric NHC proligand, **3**H[PF_6], that, in the solid state, forms a [PF_6^- ⊂ **3**H^+] host-guest system. Upon dissolution, **3**H^+ exhibits C_s-symmetry in the ^{1}H NMR spectrum. In the D_2-symmetric cation **4**, the Ag^+ ion is linearly coordinated to two **3** NHC ligands through their C2 sites. The geometries of both enantiomers **4**, namely **4**(R_a) and **4**(S_a), are stabilized by π-π intramolecular interactions, which leads to an atropisomeric behavior in solution, even at room temperature, as evidenced by ^{1}H NMR spectroscopy. Furthermore, attempts to perform transmetalation reactions at room temperature (Au(I), Cu(I)), following standard procedures[19c] were unsuccessful, highlighting the robustness of the arrangement within this compound.

Our findings indicate that, as a result of stabilizing π-π interactions, **4** exhibits a unique form of atropisomerism, due to the hindered rotation around its stereogenic C–Ag–C axis. Consequently, **4** represents an innovative example of a chiral-at-metal complex exhibiting a linear coordination geometry.

Acknowledgements

Financial support from the University of Zaragoza, the Aragón Government (A.P. predoctoral fellow, E42_23R, E05_23R), and the MCIU/AEI/FEDER (PID2021-122406NB–I00 and PID2022-137208NB–I00) is kindly acknowledged.

Conflict of Interests

The authors declare no conflict of interest.

Data Availability Statement

The data that support the findings of this study are available in the supplementary material of this article.

Keywords: Atropisomerism · Axial chirality · π-π interactions · Chiral-at-metal · NHC ligands

[1] G. P. Moss, *Pure & Appl. Chem.* **1996**, *68*, 2193–2222.
[2] a) P. Rodríguez-Salamanca, R. Fernández, V. Hornillos, J. M. Lassaletta, *Chem. Eur. J.* **2022**, *28*, e202104442; b) G. Centonze, C. Portolani, P. Righi, G. Bencivenni, *Angew. Chem. Int. Ed.* **2023**, *62*, e202303966.
[3] G. H. Christie, J. Kenner, *J. Chem. Soc., Trans.* **1922**, *121*, 614–620.
[4] a) S. T. Toenjes, J. L. Gustafson, *Future Med. Chem.* **2018**, *10*, 409–422; b) G. Bringmann, T. Gulder, T. A. M. Gulder, M. Breuning, *Chem. Rev.* **2011**, *111*, 563–639; c) C. B. Roos, C.-H. Chiang, L. A. M. Murray, D. Yang, L. Schulert, A. R. H. Narayan, *Chem. Rev.* **2023**, *123*, 10641–10727.
[5] P. W. Glunz, *Bioorg. Med. Chem. Lett.* **2018**, *28*, 53–60.
[6] a) G. Hedouin, S. Hazra, F. Gallou, S. Handa, *ACS Catal.* **2022**, *12*, 4918–4937; b) X.-F. Bai, Y.-M. Cui, J. Cao, L.-W. Xu, *Acc. Chem. Res.* **2022**, *55*, 2545–2561.
[7] a) B.-J. Wang, G.-X. Xu, Z.-W. Huang, X. Wu, X. Hong, Q.-J. Yao, B.-F. Shi, *Angew. Chem. Int. Ed.* **2022**, *61*, e202208912; b) L. Cui, H. Shinjo, T. Ichiki, K. Deyama, T. Harada, K. Ishibashi, T. Ehara, K. Miyata, K. Onda, Y. Hisaeda, T. Ono, *Angew. Chem. Int. Ed.* **2022**, *61*, e202204358; c) S. Erbas-Cakmak, D. A. Leigh, C. T. McTernan, A. L. Nussbaumer, *Chem. Rev.* **2015**, *115*, 10081–10206.
[8] a) A. Mondal, R. Toyoda, R. Costil, B. L. Feringa, *Angew. Chem. Int. Ed.* **2022**, *61*, e202206631; b) P. Zwick, A. Troncossi, S. Borsley, I. J. Vitorica-Yrezabal, D. A. Leigh, *J. Am. Chem. Soc.* **2024**, *146*, 4467–4472.
[9] a) L. Gong, M. Wenzel, E. Meggers, *Acc. Chem. Res.* **2013**, *46*, 2635–2644; b) L.-A. Chen, X. Tang, J. Xi, W. Xu, L. Gong, E. Meggers, *Angew. Chem. Int. Ed.* **2013**, *52*, 14021–14025; c) H. Huo, X. Shen, C. Wang, L. Zhang, P. Röse, L.-A. Chen, K. Harms, M. Marsch, G. Hilt, E. Meggers, *Nature* **2014**, *515*, 100–103; d) L. Zhang, E. Meggers, *Acc. Chem. Res.* **2017**, *50*, 320–330; e) L. Jarrige, Z. Zhou, M. Hemming, E. Meggers, *Angew. Chem. Int. Ed.* **2021**, *60*, 6314–6319; f) G. Wang, Z. Zhou, X. Shen, S. Ivlev, E. Meggers, *Chem. Commun.* **2020**, *56*, 7714–7717; g) P. S. Steinlandt, L. Zhang, E. Meggers, *Chem. Rev.* **2023**, *123*, 4764–4794; h) P. Xiong, S. I. Ivlev, E. Meggers, *Nat. Catal.* **2023**, *6*, 1186–1193.
[10] a) M. Chavarot, S. Ménage, O. Hamelin, F. Charnay, J. Pécaut, M. Fontecave, *Inorg. Chem.* **2003**, *42*, 4810–4816; b) E. B. Bauer, *Chem. Soc. Rev.* **2012**, *41*, 3153–3167; c) M. Carmona, R. Rodríguez, V. Passarelli, F. J. Lahoz, P. García-Orduña, D. Carmona, *J. Am. Chem. Soc.* **2018**, *140*, 912–915; d) A. G. Tejero, J. Castillo, F. Viguri, D. Carmona, V. Passarelli, F. J. Lahoz, P. García-Orduña, R. Rodríguez, *Chem. Eur. J.* **2024**, *30*, e202303935.
[11] a) R. Kubota, S. Tashiro, M. Shionoya, *Chem. Sci.* **2016**, *7*, 2217–2221; b) L.-J. Chen, H.-B. Yang, M. Shionoya, *Chem. Soc. Rev.* **2017**, *46*, 2555–2576; c) K. Endo, Y. Liu, H. Ube, K. Nagata, M. Shionoya, *Nat. Commun.* **2020**, *11*, 6263; d) X.-L. Pei, P. Zhao, H. Ube, Z. Lei, K. Nagata, M. Ehara, M. Shionoya, *J. Am. Chem. Soc.* **2022**, *144*, 2156–2163; e) S. Horiuchi, T. Yamaguchi, J. Tessarolo, H. Tanaka, E. Sakuda, Y. Arikawa, E. Meggers, G. H. Clever, K. Umakoshi, *Nat. Commun.* **2023**, *14*, 155.
[12] B. Lippert, *J. Biol. Inorg. Chem.* **2022**, *27*, 215–217.
[13] N. Lefringhausen, V. Seiffert, C. Erbacher, U. Karst, J. Müller, *Chem. Eur. J.* **2023**, *29*, e202202630.
[14] T. R. Schulte, J. J. Holstein, L. Krause, R. Michel, D. Stalke, E. Sakuda, K. Umakoshi, G. Longhi, S. Abbate, G. H. Clever, *J. Am. Chem. Soc.* **2017**, *139*, 6863–6866.
[15] S. Horiuchi, S. Moon, A. Ito, J. Tessarolo, E. Sakuda, Y. Arikawa, G. H. Clever, K. Umakoshi, *Angew. Chem. Int. Ed.* **2021**, *60*, 10654–10660.
[16] T. T. Y. Tan, F. E. Hahn, *Organometallics* **2019**, *38*, 2250–2258.
[17] Deposition numbers, 2374874 (**3**H[PF_6]·CH_3OH), 2374875(**4**[PF_6]), and 2374876 (**5**) contain the supplementary crystallographic data for this paper. These data are provided free of charge by the joint Cambridge Crystallographic Data Centre and Fachinformationszentrum Karlsruhe Access Structures service.
[18] The $head_{(C8\text{-}Theo)}$-$tail_{(C2\text{-}Im)}$-$head_{(C8\text{-}Theo)}$ orientation of heterocycles corresponds to that indicated by the green arrows at the top of Figure .
[19] a) A. Vellé, A. Cebollada, M. Iglesias, P. J. Sanz Miguel, *Inorg. Chem.* **2014**, *53*, 10654–10659; b) A. Cebollada, A. Vellé, M. Iglesias, L. B. Fullmer, S. Goberna-Ferrón, M. Nyman, P. J. Sanz Miguel, *Angew. Chem. Int. Ed.* **2015**, *54*, 12762–12766; c) A. Vellé, L. Rodríguez-Santiago, M. Sodupe, P. J. Sanz Miguel, *Chem. Eur. J.* **2020**, *26*, 997–1002.
[20] a) A. Bayler, G. A. Bowmaker, H. Schmidbaur, *Inorg. Chem.* **1996**, *35*, 5959–5960; b) A. Bayler, A. Schier, G. A. Bowmaker, H. Schmidbaur, *J. Am. Chem. Soc.* **1996**, *118*, 7006–7007.
[21] A. Vellé, A. Cebollada, R. Macías, M. Iglesias, M. Gil-Moles, P. J. Sanz Miguel, *ACS Omega* **2017**, *2*, 1392–1399.
[22] Isolated as Na[1,1′-binaphthalene-2,2′-diol-borate]·5THF (**5**), and synthesized with slight modifications as previously described:J. A. Raskatov, J. M. Brown, A. L. Thompson, *CrystEngComm* **2011**, *13*, 2923–2929.

Manuscript received: September 4, 2024
Accepted manuscript online: September 5, 2024
Version of record online: October 29, 2024